

Oceanic primary production

2. Estimation at global scale from satellite (coastal zone color scanner) chlorophyll

David Antoine, Jean-Michel André,¹ and André Morel

Laboratoire de Physique et Chimie Marines, Université Pierre et Marie Curie et CNRS, Villefranche sur Mer, France

Abstract. A fast method has been proposed [Antoine and Morel, this issue] to compute the oceanic primary production from the upper ocean chlorophyll-like pigment concentration, as it can be routinely detected by a spaceborne ocean color sensor. This method is applied here to the monthly global maps of the photosynthetic pigments that were derived from the coastal zone color scanner (CZCS) data archive [Feldman *et al.*, 1989]. The photosynthetically active radiation (PAR) field is computed from the astronomical constant and by using an atmospheric model, thereafter combined with averaged cloud information, derived from the International Satellite Cloud Climatology Project (ISCCP). The aim is to assess the seasonal evolution, as well as the spatial distribution of the photosynthetic carbon fixation within the world ocean and for a "climatological year", to the extent that both the chlorophyll information and the cloud coverage statistics actually are averages obtained over several years. The computed global annual production actually ranges between 36.5 and 45.6 Gt C yr⁻¹ according to the assumption which is made (0.8 or 1) about the ratio of active-to-total pigments (recall that chlorophyll and pheopigments are not radiometrically resolved by CZCS). The relative contributions to the global productivity of the various oceans and zonal belts are examined. By considering the hypotheses needed in such computations, the nature of the data used as inputs, and the results of the sensitivity studies, the global numbers have to be cautiously considered. Improving the reliability of the primary production estimates implies (1) new global data sets allowing a higher temporal resolution and a better coverage, (2) progress in the knowledge of physiological responses of phytoplankton and therefore refinements of the time and space dependent parameterizations of these responses.

Introduction

Photoautotrophic production by oceanic phytoplankton is a key process for the oceanic carbon cycle. Only a small fraction of the organic matter formed by photosynthesizing unicellular algae (i.e., only a fraction of the "total" primary production) is exported from the upper lighted layers of the ocean toward the deep layers (the "export production"; Eppley and Peterson, [1979]). This downward flux is however sufficient to maintain the surface CO₂ concentration lower than it would be in an abiotic ocean, as a result of the so-called "biological pump" [e.g., Sarmiento *et al.*, 1990; Antoine and Morel, 1995b]. Before attempting to estimate this depressive effect, as well as the amount of exported carbon, a prerequisite is the determination of total primary production by the algal standing stock. The knowledge of this basic process which controls the rate of inorganic carbon fixation, independently of its further fate, is essential in understanding the present carbon cycle, as well as in predicting the response of marine biota to possible changes in radiative or other physical forcing due, for instance, to global warming. The present study is specifically

devoted to the estimate of total primary production within the whole ocean, as it can be presently assessed from the first global view of the phytoplankton distribution, which is available thanks to the coastal zone color scanner (CZCS) data archive. The assessment of new and export production, out of the scope of the present study, would require additional information and specific works.

Many uncertainties still remain about the magnitude of global primary production ; published values range from about 20 to 50 Gt C yr⁻¹ (1 Gt = 10¹⁵g) [e.g., Sundquist, 1985; Berger, 1989]. In this paper it is intended (1) to demonstrate the possibility of assessing ocean primary production from satellite data, (2) to test the usefulness of a method previously developed with this aim, and (3) to examine the sensitivity of the results to various hypotheses and environmental conditions.

General Outlines of the Method

In essence, the method presently used [Antoine and Morel, this issue] allows the oceanic primary production, P, which is realized within the productive lighted layer, to be computed from the sea surface chlorophyll concentration (Chl_{sat} , mg Chl m⁻³), as detected by an ocean color sensor. The computation is based on the following global equation [Morel and Berthon, 1989] :

$$P = (1/J_C) \langle \text{Chl} \rangle_{\text{tot}} \text{PAR}(0^+) \psi^* \quad (1)$$

¹Now at Centre Orstom de Nouméa, Nouméa, Nouvelle Calédonie.

Copyright 1996 by the American Geophysical Union.

Paper number 95GB02832.
0886-6236/96/95GB-0283\$10.00

where $\langle \text{Chl} \rangle_{\text{tot}}$ represents the column integrated chlorophyll content (g Chl m^{-2}), $\text{PAR}(0^+)$ is the photosynthetically available radiant energy (within the spectral range 400-700 nm) incident at the sea level per unit area and for a given lapse of time (e.g., one day, J m^{-2}). The factor Ψ^* has the dimension of a cross section of algae for photosynthesis, per unit of areal chlorophyll biomass, and is expressed as $\text{m}^2 (\text{g Chl})^{-1}$. Note that the numerical value given to J_C , which represents the energetic equivalent of photosynthetic assimilate (expressed as $\text{kJ} (\text{g C})^{-1}$), has no numerical effect, provided that the same value is used when computing P and when generating the Ψ^* values (see below). The product $P J_C$ provides the amount of photosynthetically stored radiant energy (PSR) [Morel, 1978]. The productive layer here considered, D , exceeds in thickness that of the euphotic layer, Z_e , commonly defined as that depth where PAR is reduced to 1% of its surface value. As D extends down to the 0.1% light level, it can account for the existence of deep chlorophyll maxima, frequently, even if not systematically, located around or below Z_e . The column-integrated chlorophyll content thereafter used, $\langle \text{Chl} \rangle_{\text{tot}}$, is defined and computed as the integral of the vertical chlorophyll profile from 0 to D .

Given a Chl_{sat} concentration field derived from space observations, the computation of the photosynthetic carbon fixation rests on its pairing with "climatological" fields of the incident radiation and of the cross section Ψ^* . The Ψ^* field is preliminarily prepared and generated by systematically operating a spectral light-photosynthesis model [Morel, 1991] in various environmental conditions selected to encompass those expected when the global ocean is concerned. For fast and practical use, this field is conveniently represented by two five-dimensional lookup tables, with, as entries, the date, latitude and cloudiness index (all three determine the amount of radiant energy and its daily course), the Chl_{sat} concentration (from which $\langle \text{Chl} \rangle_{\text{tot}}$ is derived), and finally the temperature (because the physiological parameterization includes a dependence of photosynthesis upon temperature). The first table contains the Ψ^* and resulting P values computed when a uniform vertical biomass distribution is assumed; in the second table, these values are computed by assuming structured algal profiles that may include a deep chlorophyll maximum [Morel and Berthon, 1989]. These tables also contain the $\langle \text{Chl} \rangle_{\text{tot}}$ values in correspondence to each Chl_{sat} entry and the daily $\text{PAR}(0^+)$ values, stored for each date-latitude-cloudiness triplet. Therefore for each pixel within a satellite map, that is, for any given Chl_{sat} concentration, with the corresponding date and latitude, and under the proviso that cloudiness and temperature are also available (through other data sources), P is straightforwardly obtained in the lookup tables with the appropriate interpolations. In essence, this method was already applied to the western and the whole Mediterranean basins [Morel and André, 1991; Antoine et al., 1995], even if some hypotheses and parameters were different. In its presently generalized form, it is used to tentatively derive the photosynthetic carbon fixation and its month-by-month evolution at the scale of the various provinces of the world ocean.

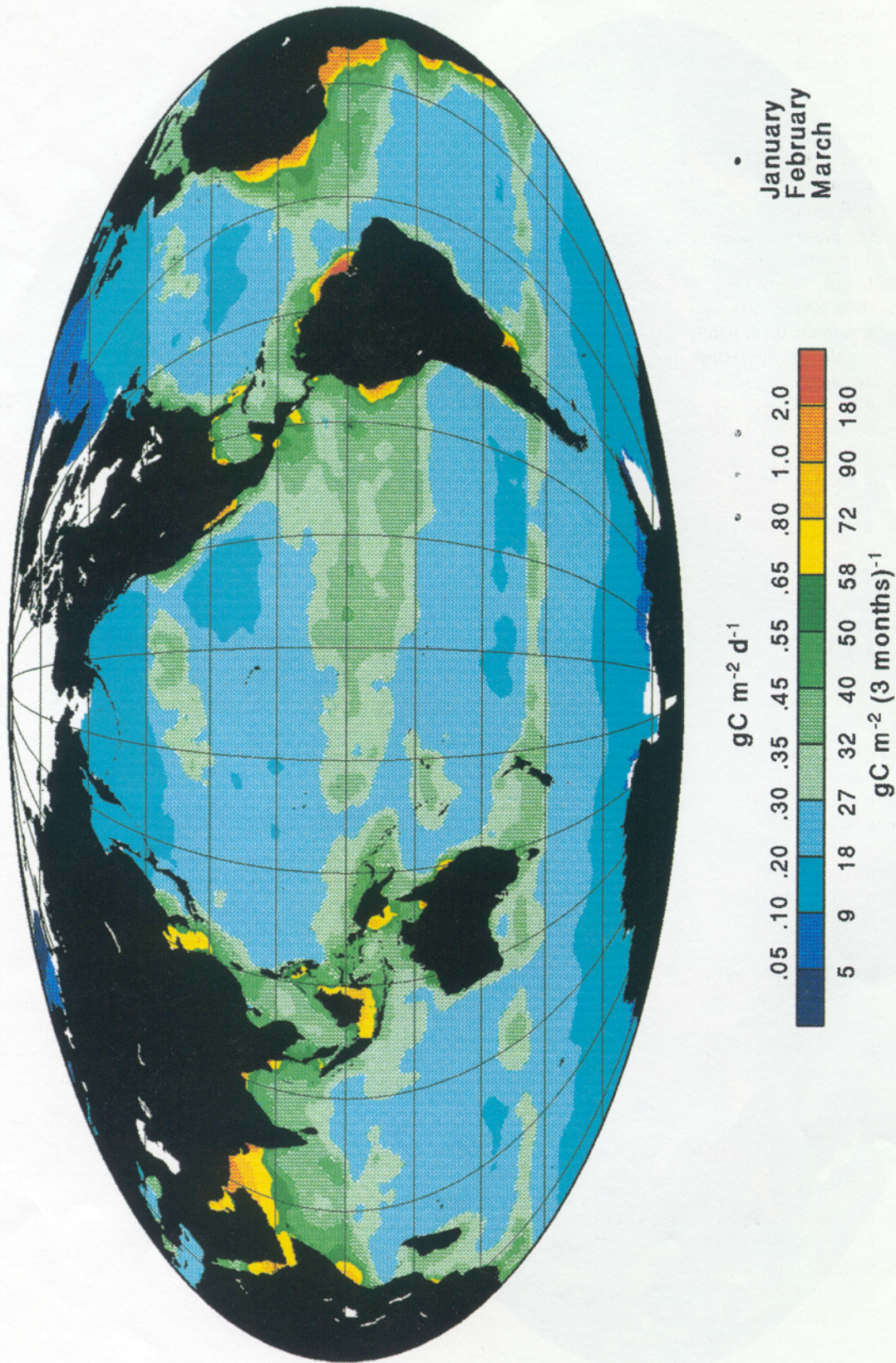
To prevent some misunderstanding about the meaning and capability of the present method, it must be recalled (see discussion by Antoine and Morel [this issue]) that such computations follow a purely diagnostic approach. The primary production actually is derived (in principle on a daily basis) from an instantaneous chlorophyll standing stock. The actual pigment content as well as its vertical distribution reflect past influences of nutrient

availability, grazing pressure, sinking, decay and physical forcing, which all have fixed and controlled the algal population at its observed level. These phenomena are in no way represented in the model itself which cannot, for this reason, be utilized as a prognostic tool in predicting the phytoplankton evolution. In practice, with the satellite data in hand for the present study, the logic of the method is somewhat twisted to cope with the lack of information on a daily basis. The chlorophyll content in each pixel must be assumed as constant over a longer period, namely over 1 month, as imposed by the availability of Chl_{sat} information in the global CZCS composite images used thereafter. It is a limitation, which is necessarily accepted for this first attempt to derive global productivity; it is anyway less severe than that resulting from the compilation of shipbound production measurements, dramatically scattered in space and time.

Basic and Ancillary Data

The 12 "climatological monthly mean" global chlorophyll images, as derived from the CZCS archive [Feldman et al., 1989] by NASA's Goddard Space Flight Center (GSFC), have been rearranged as 512x512 pixel arrays (pixel size is 78 km by 78 km at the equator, smaller at higher latitudes). Such a degraded spatial resolution, however, is much better than the resolution for the other kinds of data needed in the computation. These monthly maps, where all years (1978 until 1986) were merged, still remain incomplete because the CZCS data acquisition was not systematic, and also because some regions were persistently cloudy. The resulting coverage and sampling statistic were analyzed in a study by Yoder et al. [1993], to which the reader is referred to for further information. Simple interpolation procedures have been used to fulfill these zones where information is missing. The "correction" procedure, as developed by Yoder et al. [1993] for erroneous (i.e., overestimated) Chl_{sat} values derived at high latitudes ($> 40^\circ$), has been adopted and extended to the whole year (correction is applied for the 12 months, and not only during the 5 months centered on the winter solstice of each hemisphere). Thus the CZCS data for the high latitude belts are replaced by annual time series of chlorophyll concentration. For the southern Ocean the time series of chlorophyll at the "KERFIX" station (near Kerguelen Island in the southern Indian Ocean; M. Fiala and D. Ruiz Pino, personal communication, 1994) have been used, and for the northern hemisphere, time series at Ocean Weather Stations PAPA and INDIA have been used as by Yoder et al. [1993].

The frequency distribution of chlorophyll within the upper ocean deserves some comments. On the basis of statistical analyses of area versus chlorophyll concentration carried out in restricted zones, it has been recurrently stated that the upper layer pigment content would be spatially distributed according to (approximately) lognormal laws [Campbell and O'Reilly, 1988; Yoder et al., 1993; Campbell, 1995]. It is definitely not the case when the various oceans are globally considered and the whole range of concentrations taken into account. The distributions shown in Figure 1a (with log-log scales) are not lognormal and rather follow power laws, so that the probability of occurrence of pixels with a given Chl_{sat} concentration is always increasing when the Chl_{sat} value is decreasing (with perhaps an exception in the very low concentration domain). Interestingly, the slopes of these distributions in each ocean are not far from -1, so that the



Plates 1a-1d. Quarterly maps of primary production. Each of these maps (equal surface "Mollweide" projection) have been obtained by summing three monthly maps, as indicated, so that the units are gram of carbon per square meter and for the three months considered. For convenience, mean rates are also given in the more usual units of $\text{g C m}^{-2} \text{d}^{-1}$. Plate 1a is for the January - February - March period.

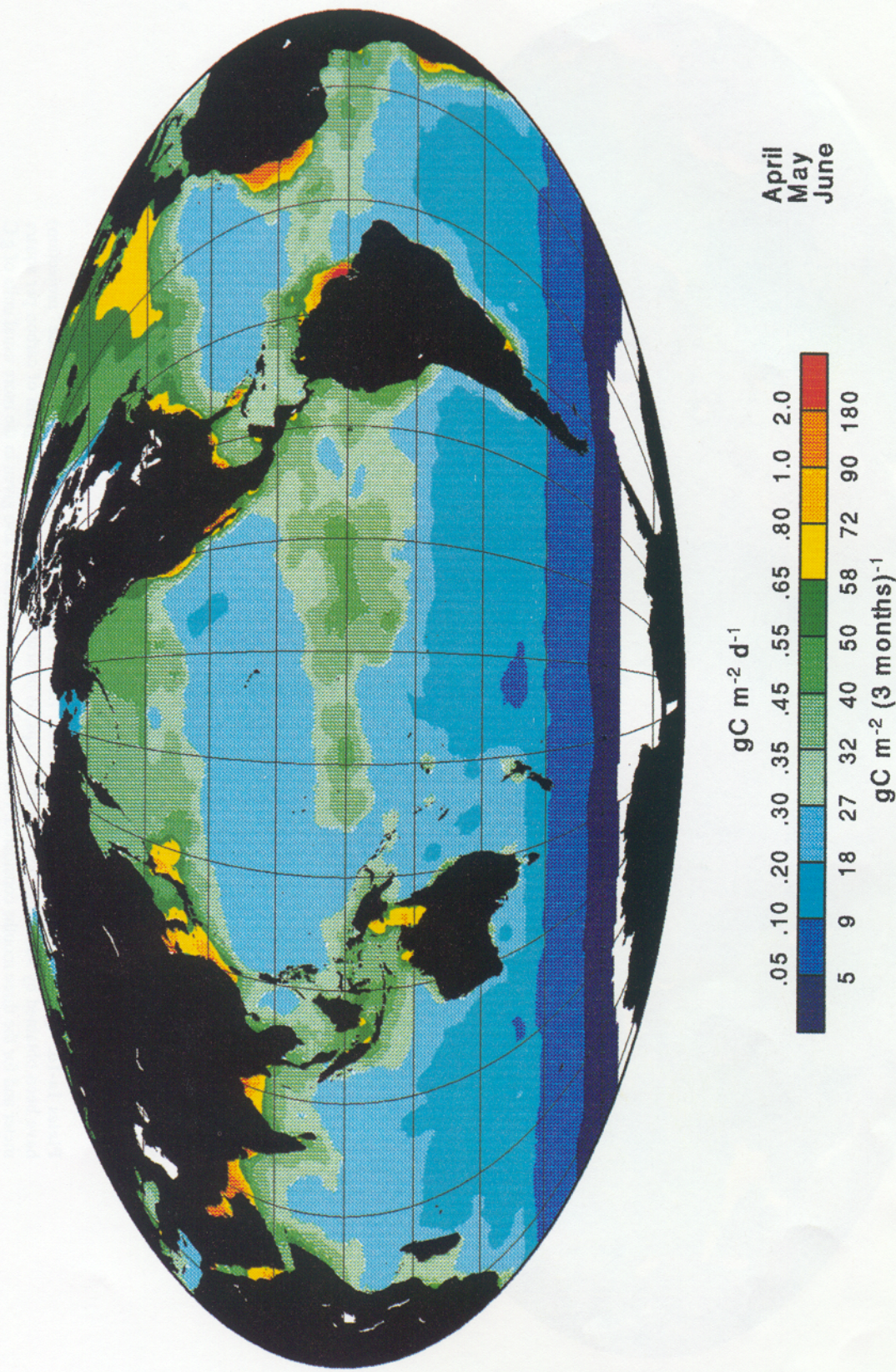


Plate 1b. As in Plate 1a, but for the April - May - June period.

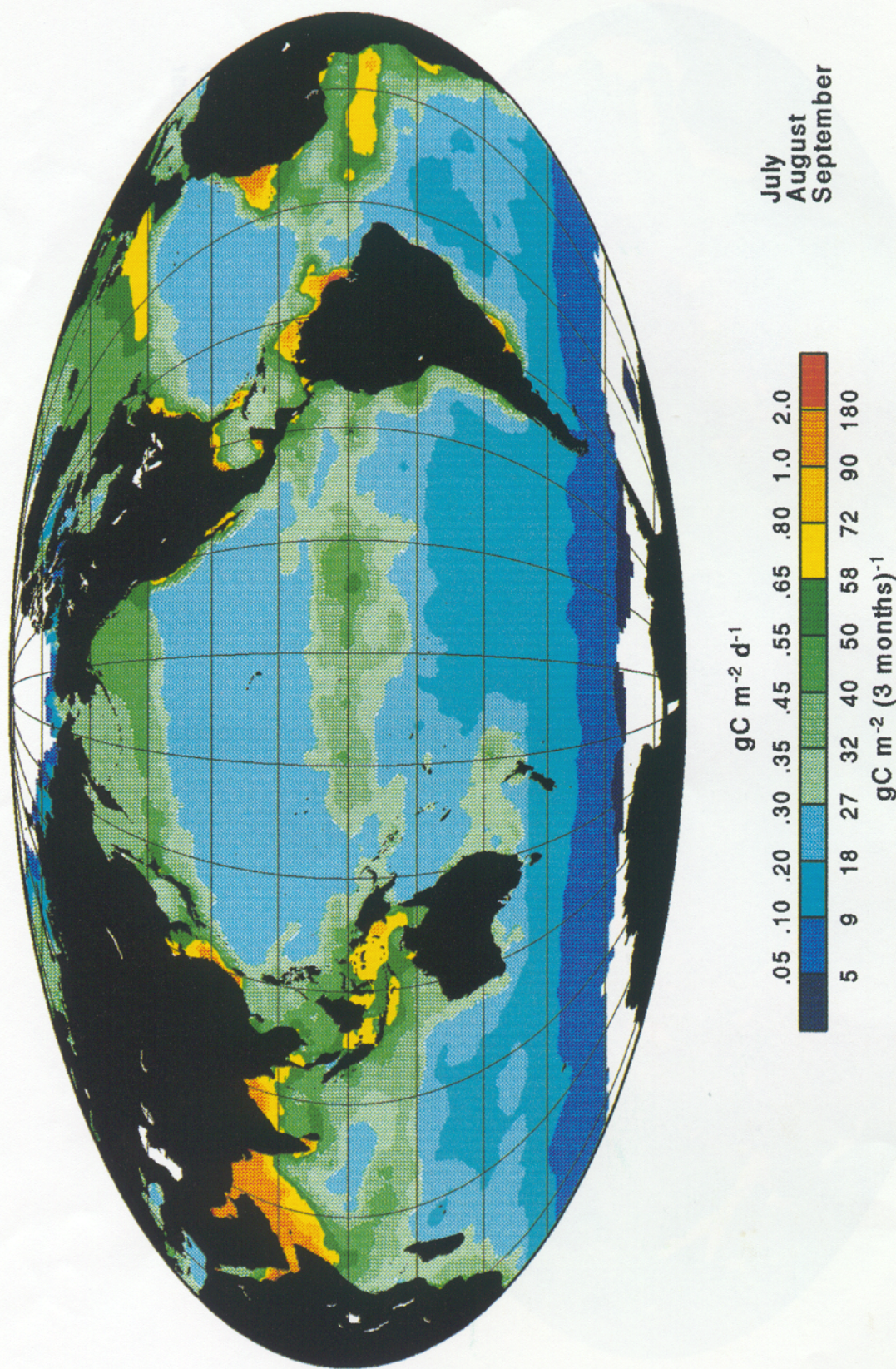


Plate 1c. As in Plate 1a, but for the July - August - September period.

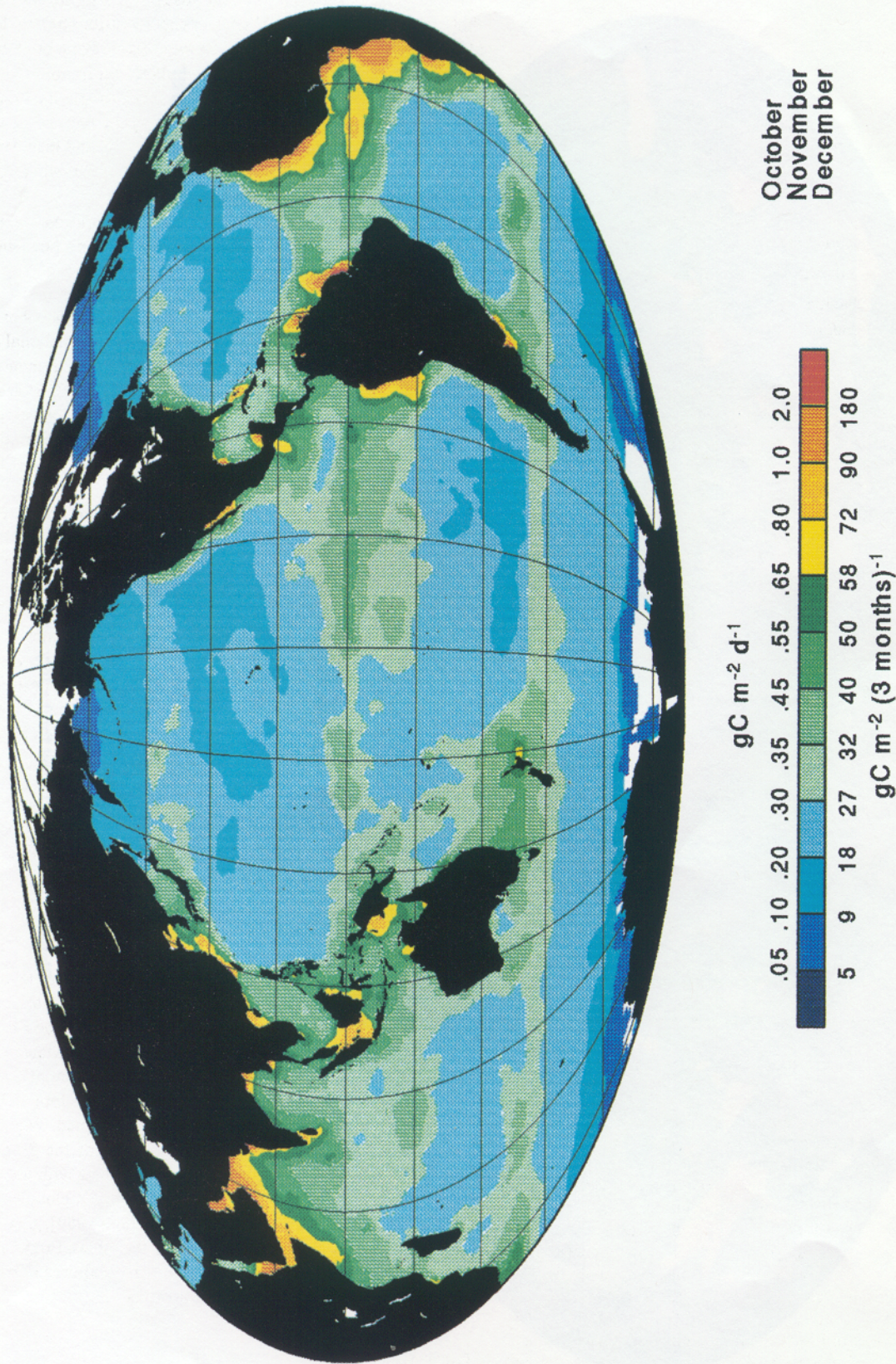


Plate 1d. As in Plate 1a, but for the October - November - December period.

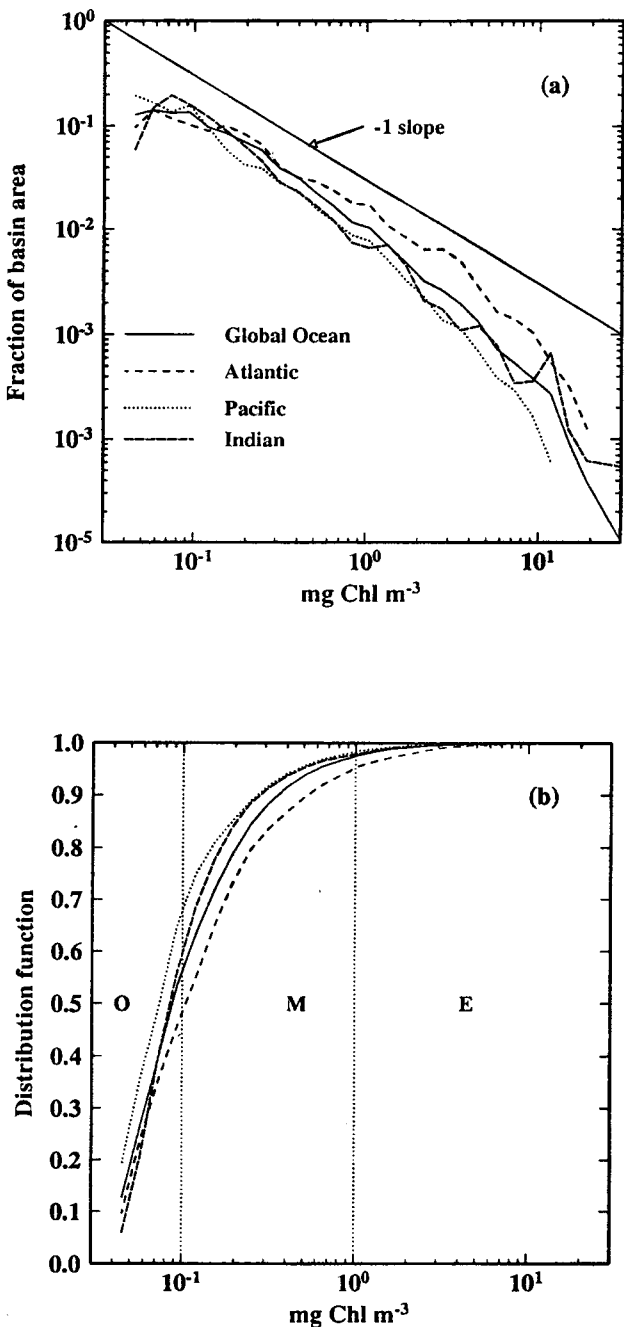


Figure 1. (a) For each ocean (and for the global ocean), fraction of the total area as a function of its upper layer chlorophyll concentration. The encoded chlorophyll values in the CZCS data set [Feldman et al., 1989] have been rearranged in such a way that 30 classes, logarithmically equal in width, encompass the 3 order of magnitude variation in chlorophyll, from 0.04 to 40 mg m^{-3} . These distributions are for the annual mean values within the 50°S - 50°N belt, and missing data are not replaced by interpolated values. The distributions for monthly mean values (not shown) are very similar (with more "noise") to those of the annual mean. (b) The fractions displayed in Figure 1a are cumulated, leading to the distribution function of chlorophyll for each ocean (and for the global ocean). The letters "O", "M", and "E" stand for oligo-, meso-, and eutrophic waters, respectively, as defined with respect to their chlorophyll content (see text and Table 2).

relative area corresponding to a given chlorophyll level is roughly inversely proportional to this level itself. This figure also shows that on the whole, the Atlantic ocean exhibits slightly higher chlorophyll concentrations than the two others. For a basin (or for the world Ocean), a "mean" chlorophyll concentration within the top layer is derived by computing the total chlorophyll content (by summing the products $\text{Chl}_{\text{sat}}(p) \cdot A(p)$ where $A(p)$ is the area of the pixel p with the concentration $\text{Chl}_{\text{sat}}(p)$), and then dividing by the total area (the sum of the $A(p)$'s). For the whole ocean, such a mean concentration is 0.19 mg m^{-3} .

The sea ice concentrations from *Walsh and Johnson* [1979] and *Zwally et al.* [1983], for the northern and southern hemispheres, respectively, are adopted to delimit the polar borders of the ocean. A $(1^\circ \times 1^\circ)$ pixel with a ice concentration higher than 50% is considered entirely icy, with no contribution to the global primary production. The cloud cover is taken from the International Satellite Cloud Climatology Project (ISCCP) data base [*Rossow et al.*, 1988], where monthly cloud indexes, on a $2.5^\circ \times 2.5^\circ$ grid, are provided for the 1983-1990 period. These data, not coincident with the CZCS data, have been averaged in view of generating 12 "climatological monthly means" of the cloud cover for the whole ocean.

Monthly values of the mixed layer depth are adopted from *Levitus* [1982]. They are used to decide whether the lookup table for uniform chlorophyll profiles (or that for stratified profiles) is the most appropriate. The adopted criteria are as follows : for high latitudes ($> 70^\circ\text{N}$, $> 45^\circ\text{S}$) the profiles are always assumed to be homogeneous, elsewhere, the hypothesis of homogeneity is also adopted as soon as the mixed layer depth, Z_{ml} , is larger than 100 m or exceeds the euphotic depth. Otherwise, the profiles are presumed to be nonuniform. On average and for the 12 months, 54% of the oceanic pixels, forming about 60% of the global ocean area, belong to the second category. It can be noted that when Chl_{sat} is greater than about 4 mg Chl m^{-3} , the vertical pigment profiles derived from statistical relationships are characterized by a broad and weak maximum near the surface (see Figure 1a by *Antoine and Morel* [this issue]). With such concentrations, the corresponding euphotic depths are less than 20-25 m. As the mixed layer often extends below this depth, such a situation finally degenerates into that of a homogeneous vertical chlorophyll profile.

At a given pixel, and once one of the two lookup tables has been selected, the Chl_{sat} value, together with the date, latitude, cloud index, and the mean temperature over the euphotic zone are the five values needed to enter into the table and extract P , with due interpolation when necessary. Because only monthly mean Chl_{sat} values are available, as well as for temperature and cloud index, the ideal day-by-day method must be adapted. When computing the monthly primary production, each of the 30 daily P values to be summed are interpolated in the tables with the appropriate dates and with the same values for Chl_{sat} , cloudiness and temperature. J_C is set to 39 kJ (g C)^{-1} [*Platt*, 1969], that is, the same value as that used when generating the tables. Producing the 12 monthly global primary production maps requires only a few minutes on a commonly available workstation.

Results

The annual course of the primary production for each of the oceans is presented in Figure 2a. The strongest seasonal signal is

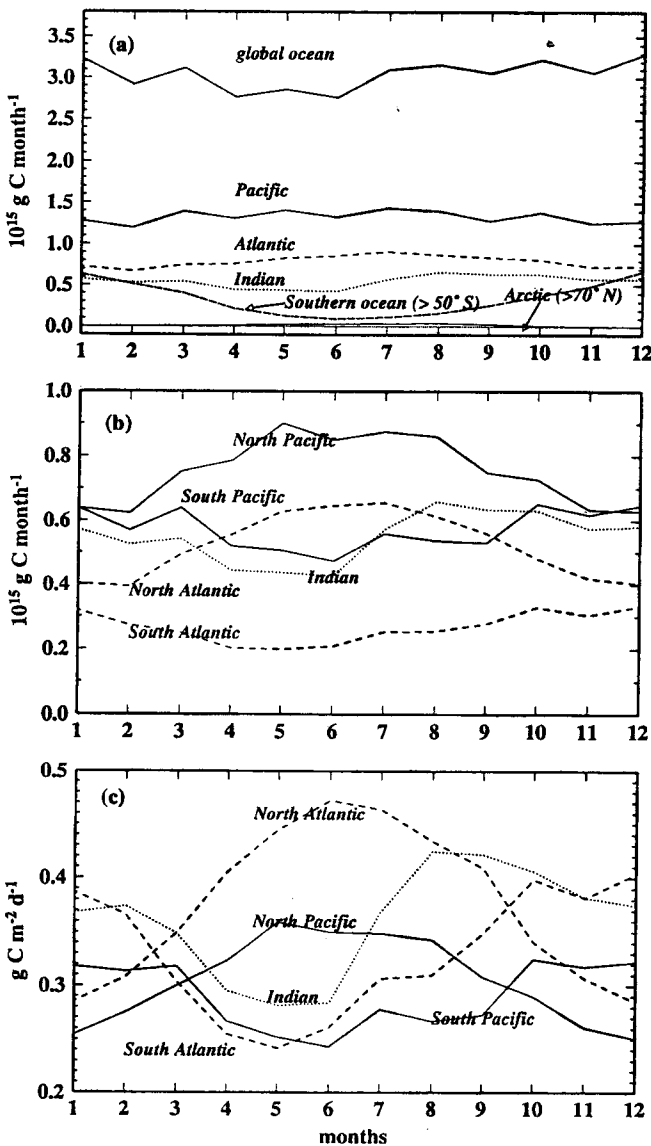


Figure 2. Temporal evolution of the primary production as integrated monthly values in the global and various oceans (a), and (b) when the oceans are split into their northern and southern basins (not for the Indian Ocean, taken as a whole). (c) as in Figure 2b, but for mean daily rates.

observed over the Arctic and Antarctic oceans ; it is obviously induced by the polar nights. The Indian ocean also exhibits a sudden increase in production triggered by the summer monsoon and the Somalia-South Arabia upwelling activity. In contrast, the Atlantic and Pacific oceans maintain a quasi-constant rate of production throughout the year as a result of the opposite seasonal variations in the two hemispheres (Figure 2b). As a rule and like other climatic signals, the seasonal signal in primary production is more accentuated in the northern than in the southern hemisphere; this is particularly true for the Atlantic ocean. In this ocean also, the daily production rate per square meter is distinctly higher (as is the chlorophyll concentration; see Figure 1a) than in the other oceanic zones. The 12 monthly primary production maps are not shown; instead quarterly maps produced by adding 3 months are

displayed (Plate 1), as well as the annual map (Figure 3). Any oceanographer can recognize the various provinces with their trophic status, and appraise the amount of details in such CZCS-based maps, compared to the broad features displayed in the historical (and non seasonal) primary production maps [e.g., *Koblenz-Mishke et al.*, 1970; *Berger*, 1989]. As a brief comment, these maps show the permanence and extension of the "blue" oligotrophic subtropical gyres ; their low production rates, however, are modulated with a slight minimum in the winter period for each hemisphere. Between these gyres, the equatorial divergence, sustaining enhanced production, is a permanent feature (except in Indian Ocean). Even with moderate biomasses, the efficiency of the equatorial belt in fixing carbon is steadily high (Table 1, column 15). In the world Ocean, the most extended high production zone is found in the northeast Indian sector during the summer monsoon. For this reason the Indian Ocean is the most productive one relatively to its area (Table 1, column 12). Vernal and summer blooms occur in both hemispheres at higher latitude. This seasonal signal is more accentuated in the northern hemisphere and affects a wide zonal band from the Arctic Ocean down to 30°N. The blooming area circles the southern hemisphere along the parallels 40-45°S and apparently does not extend poleward. Even if the low productivity derived for the Austral circumpolar Ocean is likely correct in a broad sense, more information (better temporal coverage, more accurate chlorophyll determinations, refined physiology) are definitely needed to ascertain the present, preliminary, results for this zone. The coastal upwelling systems (western coasts of Americas and Africa) are also permanent with, however, seasonal modulations and varying extensions offshore in agreement with the trade winds regime. Some anomalies can be identified in coastal zones, where turbid waters are known to prevail without being identified as such (e.g., Amazone and Orinoco plumes, Rio de la Plata, Gange delta, Yellow Sea).

According to the algorithms used in the routine processing of ocean color data [*Evans and Gordon*, 1994], turbid waters are systematically given high chlorophyll concentrations instead of being more properly identified as turbid case 2 waters. As a rule, the bias expected in turbid waters is an overestimate of the chlorophyll concentration, because of the interference with other absorbing substances (yellow substance and colored sediments or detritus). To such erroneously high chlorophyll contents will correspond anomalously large productions. In addition, when operated in turbid zones, the production model (based on the properties of case 1 waters only) predicts euphotic depth, algal absorption, and hence production superior to that realizable in turbid environments, where the radiant energy is diverted from photosynthetic utilization.

These ambiguous turbid coastal waters have not to be confounded with the high chlorophyll case 1 waters known to prevail in the major upwelling systems (off Peru, Angola, Senegal-Mauritania, Somalia-South Arabia). The status of waters in some places, as for instance inside and around the East Indian Archipelago, remains to be elucidated. This ambiguity (turbidity or chlorophyll) could be removed when processing the future sensors data by using an appropriate discriminating algorithm (some already exist, see for example, *Bricaud and Morel* [1987]). However, the quantitative assessment of chlorophyll concentrations in waters identified as case 2 waters remains a difficult issue. In open ocean there is no similar possible confusion (but

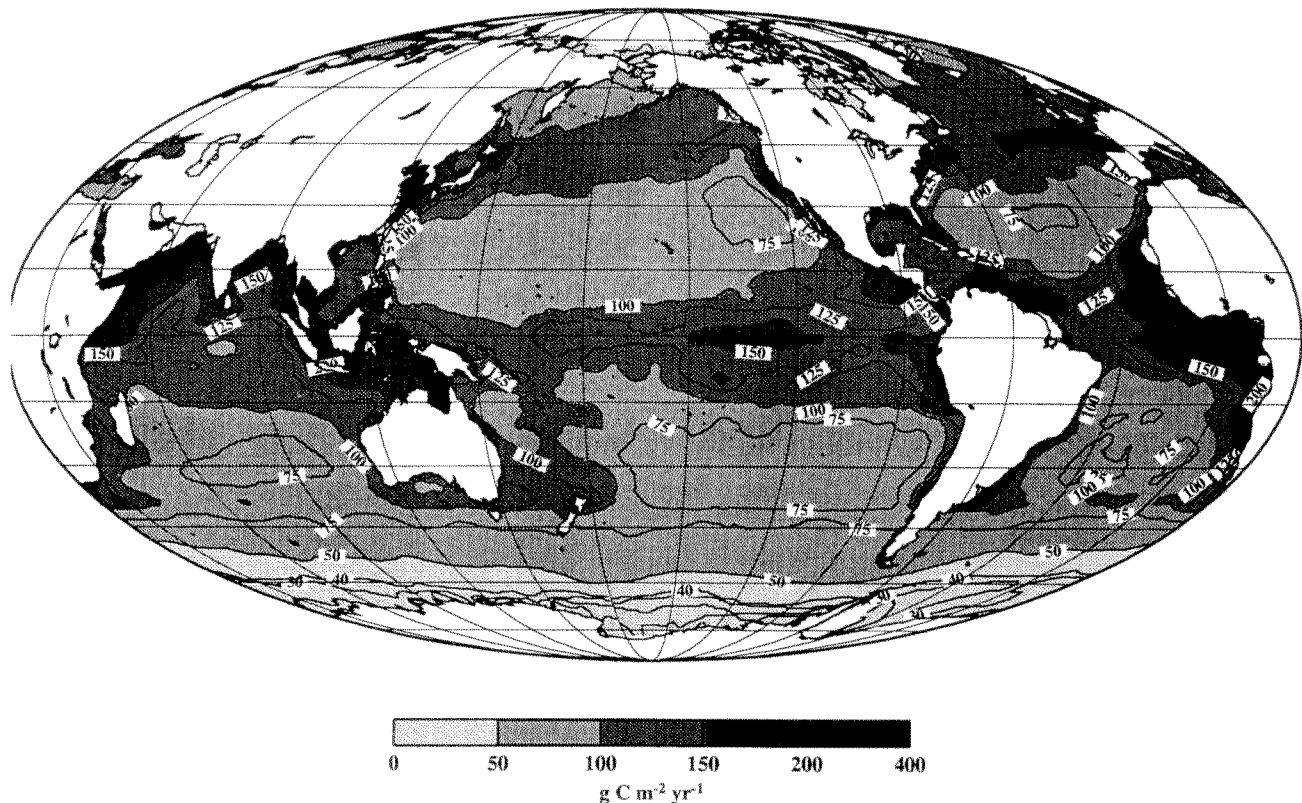


Figure 3. Annual primary production within the world ocean (equal surface “Mollweide” projection), obtained by summing the 12 monthly maps. This map shows the values obtained through the “standard” computation, which leads to a global annual carbon fixation of 36.5 Gt C yr⁻¹ (Table 1, line 1). This map can be compared to the historical primary production maps, as derived from compilations of in situ carbon fixation [e.g., Koblenz-Mishke et al., 1970; Berger et al., 1987].

Table 1. Annual Primary Production Obtained Through Various Simulations

Case	Total Production, Gt C yr ⁻¹	Percentage of Global Production							Efficiency Index						
		Atl.	Pac.	Ind.	Arc.	Ant.	Eq.	Trop.	Atl.	Pac.	Ind.	Arc.	Ant.	Eq.	Trop.
1	36.5	27.0 (9.5) [‡]	43.5 (16.0) [‡]	18.0 (6.6) [‡]	0.5 (0.18) [‡]	11.0 (4.0) [‡]	26.5 (9.7) [‡]	54.0 (19.7) [‡]	1.26	1.05	1.26	0.45	0.51	1.40	1.27
2	42.0	26.5	43.7	17.8	0.5	11.5	26.2	53.0	1.25	1.05	1.25	0.45	0.53	1.38	1.25
3	31.5	27.2	42.0	17.6	0.6	12.7	25.7	51.5	1.28	1.00	1.23	0.52	0.58	1.36	1.22
4	36.7	26.5	40.7	15.5	0.8	16.5	21.5	44.3	1.23	0.98	1.08	0.73	0.76	1.13	1.05
5	40.6	26.0	46.0	18.5	0.5	9.0	27.6	57.0	1.23	1.10	1.30	0.36	0.41	1.46	1.36

[‡] Absolute values of primary production, as Gt C yr⁻¹, in correspondance with the percentages given in line 1 and a total production equal to 36.5 Gt C yr⁻¹.

The first line (case #1) is for standard computations, the others for sensitivity experiments (cases #2 to 5, see text). The second column provides the global primary production. It is shared by the different oceanic basins and zonal belts as indicated by the percentages in columns 3 to 9. “Eq.” stands for the equatorial belt (from 10° South to 10° North), whereas “Trop.” is for the subtropical band (from 23° South to 23° North). The Antarctic ocean is delimited northward by the parallel at 50°S (approximately the mean latitude of the Antarctic convergence). The Arctic zone is delimited southward by the latitude 70°N. An “efficiency index” is given in columns 10 to 16. For a given ocean, it is defined as the ratio of its contribution to global production to its contribution to the global ocean area; it is computed as:

$$(P \text{ in the basin in question} / P \text{ in the global ocean}) / (\text{basin area} / \text{global ocean area}).$$

Therefore the average global productivity corresponds to an index equal to unity.

see below), and the major weakness of the present chlorophyll data set lies in the paucity and bad quality of the values for high latitudes, or even at moderate latitudes during winter. Coccolithophorid blooms in open ocean are also a source of misestimation of the pigment content. As they cover a very small portion of the global ocean, about 0.4% on average [Brown and Yoder, 1994], the difficulty in assessing the chlorophyll concentration in such brilliant waters is a minor drawback.

With the standard parameters adopted when producing the lookup tables [Antoine and Morel, this issue], the total annual primary production amounts to 36.5 Gt C yr⁻¹. This value is obtained when assuming that ρ , the ratio of active chlorophyll to the sum of active and degraded pigments (chlorophyll and pheopigments) is 0.8. This average value estimated by Morel and Berthon [1989] was based on old determinations of pigments via the spectrophotometric or fluorimetric method. According to recent determinations (via high pressure liquid chromatography technique), the relative pheopigment contribution appears much lower than previously estimated [Claustre and Marty, 1995]. Therefore if ρ is assumed to reach its upper limit (unity), the resulting production would be 45.6 Gt C yr⁻¹. This global production is shared by the three oceans and the two polar regions according to relative contributions and absolute values which are provided in Table 1 (lines 1 and 2, respectively).

Discussion : Sensitivity Tests

With respect to the above results, various numerical experiments can be carried out, in view of understanding the importance of several environmental factors or of unavoidable uncertainties in parameterizations.

1. If the cloudiness is withdrawn, the global production for the same algal biomass would be increased by only 15% (line 2). It is conceivable that the actual cloud cover (on average about 40% over the oceans) does not entail a considerable reduction of the primary production as its impact on Ψ^* is not linear (Figure 25 by Morel [1991]). The formulation adopted to express the radiation attenuation by clouds perhaps tends to overestimate irradiance for overcast conditions [Bishop and Rossow, 1991], and thus the production values in presence of clouds would be too high. According to the above test, however, this overestimation cannot have a significant influence.

2. If the deep algal biomass maxima in stratified waters are disregarded, and thus if the Ψ^* values for all pixels are taken in the table for uniform profiles (Chl_{sat} whatever the depth), the resulting production is lowered by 14% (line 3). This change demonstrates the need for considering the layer extending from the 1% to the 0.1% light levels, which often includes a more or less important part of the deep chlorophyll maximum. The above number is also interesting in that it fixes the relative uncertainty that would result from failures when sorting out the deep mixed and the stratified situations, or from deficiencies in representing the shape and magnitude of the deep chlorophyll maxima. When discriminating between the two kind of situations, an a priori oceanographic knowledge as well as a monitoring of the sea surface temperature evolution can prevent from making at least significant errors in the sorting process. In another sensitivity analysis [Antoine and Morel, this issue], it was also shown that, instead of annihilating the deep chlorophyll maximum as above,

doubling its intensity (with respect to its statistical mean value) has only a negligible effect.

3. According to the sensitivity tests [Antoine and Morel, this issue], a change in the maximum light-saturated photosynthetic rate per unit of biomass, P^B_{\max} , is the most important cause of change in Ψ^* and P , with respect to their values produced by the standard model. In this model, there is a unique value for P^B_{\max} , namely 4.6 g C g Chl⁻¹ h⁻¹ at 20°C, leading to a unique P^B_{\max} temperature relationship (modelled according to Eppley [1972]). A unique relationship is likely oversimplifying when applied to the global ocean and all algal populations as it ignores possible acclimation. A completely achieved thermal acclimation would be represented by situations where P^B_{\max} would become constant and independent from temperature. There is no physiological basis for such an independence and proofs of the contrary exist [Gilstad and Sakshaug, 1990]. Nevertheless, such a hypothetical full acclimation can form an extreme case for a numerical experiment. The simulation is straightforward as it suffices to run the code by using everywhere the Ψ^* value for a single temperature. The mean upper ocean temperature as computed from the Levitus atlas, namely 18.1 °C, is used for simulating this hypothetical full acclimation. In correspondance P^B_{\max} is 4.1 g C (g Chl)⁻¹ h⁻¹, for all algal populations whatever the oceanic zone and the surrounding temperature. The result of this trial (line 4 in Table 1) is somewhat surprising as the final value of the global production remains nearly unchanged. This fortuitous result obviously is the consequence of compensating effects; the primary production is approximately doubled in the Arctic and Antarctic zones, and in the meanwhile the tropical belt becomes less productive, by about 25% (see Figure 4a). Therefore the above numerical result, relative to the global ocean, is in no way valid at regional scale. If information about P^B_{\max} are available for specific bio geographical provinces [e.g., Platt et al., 1991], it must and can be used. For that purpose there is no need to generate new tables, and the present lookup tables can still be used. Since there is a unique and monotonous relationship between P^B_{\max} and temperature (equations (A7) and (A8), Antoine and Morel [this issue]), it suffices to enter with the appropriate temperature (differing from the actual one) in order to obtain the desired P^B_{\max} values.

4. The Levitus temperature atlas was used in the standard computation. Actually a mean temperature was computed for the euphotic layer (Z_e) and then considered as unchanged down to D ($\approx 1.5 Z_e$). Such a mean temperature is probably too high for the deeper layer (Z_e to D), however the amount of carbon fixed is admittedly low in this deep zone. In contrast, this mean temperature is likely too low for the top layers, generally warmer than the average temperature of the euphotic zone. This is a limitation of the present method, because it cannot be envisaged, at least in a simple way, to produce tables by running the model with vertically varying temperature throughout the productive layer. The impact of the constant temperature assumption cannot be tested without abandoning the use of tables. It is thus necessary to operate the full model at the pixel level and to introduce the temperature profiles as found in Levitus (for each 1° x 1° domain). The results of this detailed computation are shown in Table 1, line 5. With respect to the standard computation (line 1), there is a raise of the global production (by about 11%), which, as expected, originates from enhanced values in the 30°S to 30°N zonal belt (Figure 4b). The need for considering the temperature vertical structure in future algorithms remains open to discussion.

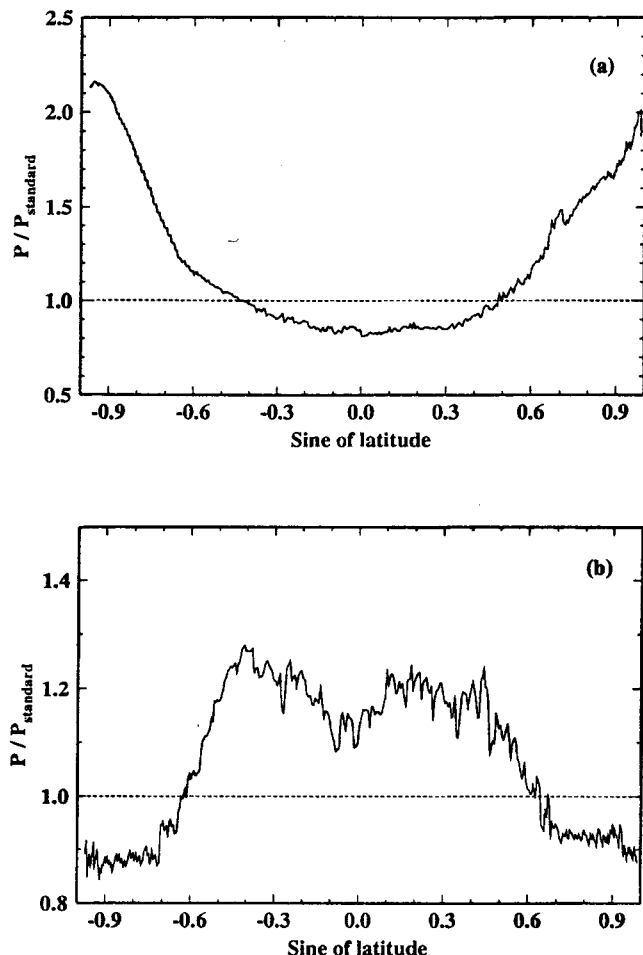


Figure 4. (a) The ratio of the mean zonal primary production rates, derived under the hypothesis of complete adaptation to temperature (Table 1, line 4), to the rates obtained in the standard simulation (Table 1, line 1). (b) The ratio of the mean zonal primary production rates, computed when the vertical temperature profile is taken into account (Table 1, line 5), to the rates obtained in the standard simulation (Table 1, line 1).

Discussion : Global Primary Production Values

Considering the annual CZCS chlorophyll map, the mean concentration within the upper layer of the ocean amounts to $0.19 \text{ mg Chl m}^{-3}$. Month-to-month variations in this value are insignificant because of the inter hemispheric seasonal compensations. To this mean surface concentration corresponds a mean vertically integrated chlorophyll content of about $24.6 \text{ mg Chl m}^{-2}$. It has generally been admitted that the typical error associated with satellite-derived chlorophyll concentration would be of the order of $\pm 35\%$ for open ocean case 1 waters [e.g., *Gordon and Morel, 1983*]. Because the vertically integrated biomass roughly varies as the square root of the surface concentration (Figure 10 by *Morel [1991]* and Figure 1b by *Antoine and Morel* [this issue]), the uncertainty in $\langle \text{Chl} \rangle_{\text{tot}}$ is about $\pm 17\%$. Therefore the uncertainty in P only attributable to errors in the satellite chlorophyll (and when everything else is kept unchanged) is of the same order and about $\pm 17\%$.

By integrating over the entire ocean, it appears that the global chlorophyll standing stock is weakly variable along the seasons

($\pm 5\%$), and amounts to about $8.6 \cdot 10^{12} \text{ g Chl}$ when the whole productive layer (down to D) is considered. By assuming a carbon-to-chlorophyll ratio of 100, the algal reservoir in terms of carbon would be 0.86 Gt C . With the annual carbon fluxes provided in Table 1, the mean residence time of carbon within this reservoir would be as short as 1 week on average.

Equation (1) can be operated on a global scale. With the cloud climatology presently used, the photosynthetically available radiation at the ocean surface, $\text{PAR}(0^\circ)$, is on average 29 PW ($1 \text{ PW} = 10^{15} \text{ W}$). When combined with the $\langle \text{Chl} \rangle_{\text{tot}}$ value given above ($8.6 \cdot 10^{12} \text{ g Chl}$) and with the computed carbon fixation ($36.5 \text{ Gt C yr}^{-1}$, corresponding to $\text{PSR} = 0.0453 \text{ PW}$), equation (1) can be solved for Ψ^* . The resulting Ψ^* value is $0.08 \text{ m}^2 (\text{g Chl})^{-1}$, and Ψ , the light utilization index (sensu *Falkowski [1981]*) is about $50 \text{ g C} (\text{g Chl})^{-1} (\text{mol photon m}^{-2})^{-1}$. The ratio of PSR to PAR is about 0.16% , whereas PAR forms about 45% of the solar radiation at the sea level. Therefore it turns out that 0.07% of the solar energy is regularly captured by the algal compartment and then regularly fuels the food chain and other biogeochemical processes occurring in the ocean interior. This estimate of the radiation utilization by phytoplankton is close to one third of that attributed on average to the terrestrial phytosphere (see for example, *Budyko [1974]*).

In a famous paper, *Ryther [1969]* assigned specific levels of primary production to different parts of the ocean. According to his division (his Table 2), the richest parts of the ocean (coastal zones, upwelling areas, and offshore regions of high production), which amount to 10% of the total oceanic area, would contribute to 20% of the global primary production (global production is estimated at 20 Gt C yr^{-1} by Ryther). In contrast, and in spite of a reduced productivity rate, the open ocean (90% of the total area) still would support 80% of the total production. These figures proposed by Ryther are to be compared to those extracted from the global annual map (Figure 3) and recorded in Table 2. A division into three ecological provinces is here adopted on the basis of their mean annual chlorophyll content (see Figure 1b). Rather than geography, these provinces reflect a mean trophic status (oligo-, meso-, and eutrophic conditions). As the satellite chlorophyll data are incomplete and questionable for high latitudes, only the 50°S to 50°N belt has been considered in this

Table 2. Division of the Ocean Into Provinces According to Their Annual Mean Levels of Chlorophyll Concentration in the Upper Layer

Province	Chlorophyll mg m^{-3}	Area (%)	Production		
			%	Gt C yr^{-1}	$\text{g C m}^{-2} \text{ yr}^{-1}$
Oligotrophic	$\text{Chl} \leq 0.1$	55.8	44.0	14.5	91.0
Mesotrophic	$0.1 < \text{Chl} \leq 1$	41.8	47.5	15.7	131.5
Eutrophic	$\text{Chl} > 1$	2.4	8.5	2.8	422.0
Total		100	100	33.0	

Only the 50°S to 50°N zonal belt is considered here, thus the total area actually represents 81% of the entire ocean and the total production represents 91% of the production of the entire ocean (line 1 in Table 1). The contributions of the three provinces to the total production are given (in relative and absolute units), as well as their productivity per unit of area.

analysis. Because this belt represents as much as 81% of the total oceanic area and contributes to about 91% of the total primary production, such an analysis still remains significant. Within this belt, a very small fraction, about 2.4% in area, exhibits chlorophyll concentration higher than 1 mg m^{-3} , and contributes to about 8% of the total primary production. This contribution is probably overestimated, to the extent that some turbid case 2 waters (erroneously accounted for as chlorophyll rich and thus highly productive waters) are included within this category. The oligotrophic and mesotrophic provinces (forming together 97.6% of the total oceanic area) roughly coincide with the "open ocean" (*sensu Ryther* [1969]). Their predominance in the photosynthetic carbon fixation process (92% of the total primary production), already emphasized by Ryther, is confirmed and even reinforced by the present analysis. The mesotrophic and oligotrophic provinces are approximately of equal importance in terms of global productivity.

Conclusion

This study, based on the presently available CZCS pigment imagery, is intended both to demonstrate in a real case the applicability of a method resting on the use of precomputed climatological lookup tables [Antoine and Morel, this issue], and to produce a renewed picture of the primary production within the world ocean. Owing to the method and the data used, this picture is considerably more detailed than that given by previously published maps, with respect to the spatial and temporal resolution. The global or local primary production computation, however, is heavily depending on values assigned to several crucial physiological and ecological parameters. Of prime importance are the parameters of the P versus E curve [Antoine and Morel, this issue]. Also, the value adopted for the activity index ρ directly reacts on the computed production. As demonstrated by the sensitivity studies in the above reference, some other processes, intuitively believed to have rather large impacts on the primary production prediction, prove to be less important, as the spectral shape of algal absorption, photoinhibition, and more unexpectedly the vertical structure of the algal biomass. Even the temperature adaptation capacity, if actually existing, would not deeply alter the annual world ocean primary production, provided that a reasonable temperature dependency is accounted for in the computation. It must be stressed again that, in spite of a rather accurate physical modelling, and of the enormous amount of information about the algal biomass obtainable from space, the derivation of the primary production can only become more accurate in the future if considerable progress is made about the algal ecology and physiology, at the required spatial and temporal scale. The insufficient spatial and temporal coverage by the CZCS sensor, the relatively poor quality of the data for polar zones, and the remaining ambiguities for many coastal zones, when retrieving their pigment concentration, are other drawbacks, which hopefully will be removed thanks to the next generation of satellite borne sensors.

The absolute values of the global primary production found here are among the highest estimates previously proposed from various compilations of *in situ* data (from Koblenz-Mischke [1970] to Berger [1989]). If the present results remain somewhat questionable in absolute values, the relative contribution of the various zonal belts and oceans to the global production are very

likely well described, as well as the geographical patterns with their seasonal evolutions. The restrictions to bear in mind concerning the tentative values presented here originate from the coarse spatial and temporal resolution of the climatological fields presently available and combined. The present exercise, where the chlorophyll maps merge 6 years, where cloudiness maps merge three other years, where all factors are assumed to be constant for 1 month durations, can appear as an academic one. In some sense, it is true, and the final numbers are probably less important than the way of deriving them, which demonstrate the feasibility of assimilating more precise and frequent data. The use of precomputed lookup tables on a routine basis is well adapted to the future sensor data rate and efficient in terms of computational effort. Ocean primary productivity could be routinely computed at a temporal resolution (week ?), which still remains to be analyzed, as well as optimized, by considering both the time rate of physical and biological changes and the time rate of delivery of the necessary data. These data include not only the chlorophyllous pigments but also the cloud coverage, sea surface temperature, and dynamics of the mixed layer.

Acknowledgments. The authors would like to express their appreciation to two anonymous reviewers for valuable criticism and suggestions. We acknowledge support of the European community, through the contract ESCOBA-EV5V-CT92-0124.

References

- Antoine, D., and A. Morel, Oceanic primary production. I, Adaptation of a spectral light-photosynthesis model in view of application to satellite chlorophyll observations, *Global Biogeochem. Cycles*, this issue.
- Antoine, D., and A. Morel, Modelling the seasonal course of the upper-ocean pCO_2 , II, Validation of the model and sensitivity studies, *Tellus*, **47B**, 122-144, 1995b.
- Antoine, D., A. Morel, and J. M. André, Algal pigment distribution and primary production in the eastern Mediterranean as derived from coastal zone color scanner observations, *J. Geophys. Res.*, **100**, 16,193-16,209, 1995.
- Berger, W. H., Global maps of ocean productivity, in *Productivity of the Ocean : Present and Past*, edited by W.H. Berger, V.S. Stemacek, and G. Wefer, pp. 429-455, John Wiley, New-York, 1989.
- Bishop, J. K. B., and W. B. Rossow, Spatial and temporal variability of global surface solar irradiance, *J. Geophys. Res.*, **96**, 16,839-16,858, 1991.
- Bricaud, A., and A. Morel, Atmospheric corrections and interpretation of marine radiances in CZCS imagery : Use of a reflectance model, *Oceanol. Acta*, **7**, 33-50, 1987.
- Brown C. W., and J.A. Yoder, Coccolithophorid blooms in the global ocean, *J. Geophys. Res.*, **99**, 7467-7482, 1994.
- Budyko, M. I., *Climate and Life*, Int. Geophys. Ser., edited by D.H. Miller, vol. 18, 508pp., Academic, San Diego, Calif., 1974.
- Campbell, J. W., The lognormal distribution as a model for bio-optical variability in the sea, *J. Geophys. Res.*, **100**, 13237-13254, 1995.
- Campbell, J. W., and J. E. O'Reilly, Role of satellites in estimating primary productivity on the northwest Atlantic continental shelf, *Cont. Shelf Res.*, **8**, 179-204, 1988.
- Claustre, H., and J. C. Marty, Specific phytoplankton biomasses and their relation to primary production in the tropical north Atlantic, *Deep Sea Res.*, in press, 1995.
- Eppley, R. W., Temperature and phytoplankton growth in the sea, *Fish. Bull.*, **70**, 1063-1084, 1972.
- Eppley, R. W., and B. J. Peterson, Particulate organic matter flux and planktonic new production in the deep ocean, *Nature*, **282**, 677-680, 1979.
- Evans, R. H., and H. R. Gordon, coastal zone color scanner "system calibration" : A retrospective examination, *J. Geophys. Res.*, **99**, 7293-7307, 1994.

- Falkowski, P. G., Light-shade adaptation and assimilation numbers, *J. Plank. Res.*, 3, 203-216, 1981.
- Feldman, G. C., et al., Ocean color : Availability of the global data set, *Eos Trans. AGU*, 70, 634, 1989.
- Gilstad, M., and E. Sakshaug, Growth rates of ten diatoms species from the Barents sea at different irradiances and day lengths, *Mar. Ecol. Prog. Ser.*, 64, 169-173, 1990.
- Gordon H. R., and A. Morel, Remote assessment of ocean color for interpretation of satellite visible imagery, edited by R.T. Barber, C.N.K. Mooers, M.J. Bowman, and B. Zeitzschel, 114 pp., Lecture notes on coastal and estuarine studies, 4, 1983.
- Koblenz-Mishke, O. I., V. V. Volkovinsky, and J. G. Kabanova, Plankton primary production of the world ocean, in *Scientific Exploration of the South Pacific*, edited by W. Wooster, pp. 183-193, Nat. Acad. Sci., Washington, D.C., 1970.
- Levitus, S., Climatological atlas of the world ocean, U.S. Govt. Print. Off., Washington D.C., *NOAA Prof. Pap.*, 13, 1982.
- Morel, A., Available, usable, and stored radiant energy in relation to marine photosynthesis, *Deep Sea Res.*, 25, 673-688, 1978.
- Morel, A., Light and marine photosynthesis: A spectral model with geochemical and climatological implications, *Prog. Oceanogr.*, 26, 263-306, 1991.
- Morel, A., and J. M. André, Pigment distribution and primary production in the western Mediterranean as derived and modeled from coastal zone color scanner observations, *J. Geophys. Res.*, 96, 12,685-12,698, 1991.
- Morel, A., and J. F. Berthon, Surface pigments, algal biomass profiles, and potential production of the euphotic layer: Relationships reinvestigated in view of remote-sensing applications, *Limnol. Oceanogr.*, 34, 1545-1562, 1989.
- Platt, T., The concept of energy efficiency in primary production, *Limnol. Oceanogr.*, 14, 653-659, 1969.
- Platt, T., C. Caverhill, and S. Sathyendranath, Basin-scale estimates of oceanic primary production by remote sensing: The North Atlantic, *J. Geophys. Res.*, 96, 15,147-15,159, 1991.
- Rossow, W. B., L. C. Carder, P. J. Lu, and A. W. Walker, International Satellite Cloud Climatology Project (ISCCP) documentation of cloud data, 1988.
- Ryther, J. H., Photosynthesis and fish production in the sea, *Science*, 166, 72-76, 1969.
- Sarmiento, J. L., G. Thiele, R. M. Key, and W. S. Moore, Oxygen and nitrate new production and remineralization in the North Atlantic subtropical gyre, *J. Geophys. Res.*, 95, 18,303-18,315, 1990.
- Sundquist E. T., Geological perspectives on carbon dioxide and the carbon cycle, in *The carbon cycle and atmospheric CO₂: Natural variations archean to present*, edited by E.T. Sundquist and W.S. Broecker, pp. 5-59, Washington D. C., 1985.
- Walsh, J. E., and C. M. Johnson, Interannual atmospheric variability and associated fluctuations in Arctic sea ice extent, *J. Geophys. Res.*, 84, 6915-6928, 1979.
- Yoder, A. Y., C. R. McClain, G. C. Feldman, and W. E. Esaias, Annual cycles of phytoplankton chlorophyll concentrations in the global ocean: A satellite view, *Global Biogeochem. Cycles*, 7, 181-193, 1993.
- Zwally, H. J., J. C. Comiso, C. L. Parkinson, W. J. Campbell, F. D. Carsey, and P. Gloersen, Antarctic sea-ice, 1973-1976: Satellite passive-microwave observations, Washington D. C., *NASA Spec. Publ.*, 459, 1983.
-
- D. Antoine and A. Morel, Laboratoire de Physique et Chimie Marines, Université Pierre et Marie Curie et CNRS, BP 8, Quai de la Darse, F 06230, Villefranche sur Mer, France. (e-mail : david@ccrv.obs-vlfr.fr ; morel@ccrv.obs-vlfr.fr)
- J. M. André, Centre Orstom de Nouméa, BP A5, Nouméa cedex, Nouvelle Calédonie (e-mail: andre@noumea.orstom.nc)

(Received October 28, 1994; revised September 8, 1995; accepted September 13, 1995.)